Original Article

Mechanical properties and fire-resistance of composites with marble particles

Juana Abenojar [a,c,], Miguel-Angel Martínez [a], Sara López de Armentia [b], Eva Paz [b], Juan-Carlos del Real [b], Francisco Velasco [a]*

[a] Materials Science and Engineering and Chemical Engineering Department, In-service Material Performance Group, "Álvaro Alonso Barba" Institute of Chemistry and Materials Technology, Universidad Carlos III de Madrid, Av. Universidad, 30-28911, Leganés, Spain
[b] Institute for Research in Technology/Mechanical Engineering Department, Universidad Pontificia Comillas, Alberto Aguilera 25, 28015 Madrid, Spain
[c] Mechanical Engineering Department, Universidad Pontificia Comillas, Alberto Aguilera 25, 28015 Madrid, Spain

ARTICLE INFO

ABSTRACT

The main aim of this work is to manufacture a composite material based on a natural material (marble) with acceptable mechanical properties and fire resistance, for being used in habitat industry as floor or wall in buildings. Marble used as raw material is the waste powder of quarry or plate manufacturing. To achieve this objective, polyester matrix composites with 50 wt.% of marble and 3 wt.% of glass fiber (short fiber or mesh) were prepared. The novelty of this study is the high percentage of ceramic material added to a polymer matrix composite and the fire resistance study. Samples were characterized mechanically through flexural test, Charpy impact test, compression test and wear resistance by pin-on-disk test. Fracture surfaces were analyzed by scanning electron microscope (SEM), and wear tracks were studied by SEM and 3D optical profilometer. Besides, samples were subjected to fire test using a Bunsen burner at 900 °C for 20 min. Sample temperature at the opposite-to-fire test side was measured with an infrared thermometer. Results show that marble improves mechanical properties of polyester and the effect of the glass fiber depends on its morphology (fiber or mesh). Fire resistance is high, and the fire goes out when the flame is turned off. Furthermore, the mesh maintains the integrity of the sample.

1. Introduction

Ablative materials act as heat shields since they are able to dissipate considerable amounts of heat through different

physical-chemical phenomena: chemical reactions, vaporization and sublimation [1]. Ablation comes from a geological term meaning "to carry away". Mainly, two kind of ablative materials may be distinguished: polymer ablatives (organic polymers and composites), and non-polymer ablatives (inorganic polymers/oxides and metals) [2]. In the case of polymer materials, pyrolysis reaction leads to the release of gas species and the formation of brittle carbonaceous solid products (char) due to the decomposition of organic compounds. Thanks to their endothermic character, these reactions absorb part of the incoming heat. Furthermore, pyrolysis gases flow and reduce the incident convective flux in the interface, providing convective cooling.

Failure of ablative materials may occur following different mechanisms [3]:

- Char spallation: the formed porous char layer is subjected to high stresses related to pressure and thermal gradients. In this process, mass is lost without accommodating much energy.
- Flow of glassy liquid layer: in materials containing significant amounts of glass in its composition, a glassy liquid layer is formed with an ablative effect: its vaporization absorbs a significant amount of heat. However, if this layer is exposed to shear, it can flow and the underlying material is suddenly exposed, which results in rapid erosion.

The concept of ablative materials, widely used in aerospace, can be transferred to other technological fields taking advantage of the decomposition into charred material and the formation of gaseous products. The use of different polymeric matrices, instead of typical phenolics, and the selection of proper reinforcements can lead to new applications, where different requirements are needed. Unsaturated polyester resin (UPE) has been widely used across the construction industry (flat roofing and floors, guttering, pool floors, etc.) thanks to its good mechanical properties including compression strength [4], water resistance, and resistance to alkalis [5]. The solvent absorptions of UPE are lower in alkali solutions than in water, and also less than in epoxy resin [5]. Additionally, UPE has already been used as ablative material, thanks to its charring characteristics [6]. However, this resin presents low fire resistance and burns with heavy smoke and soot. To expand the use of this resin, its flame retardation, thermostability, and glass transition temperature must be improved [7].

To improve the fire resistance of polymers, some reinforcements or fillers are usually included in their composition. Halogenated flame retardants have been conventionally used to increase fire resistance with good results; however, they emit toxic dioxins during their combustion [8]. Other flame retardant additives affect some properties, like thermal stability, mechanical stability, curing behavior and water resistance [9–11]. As an alternative, some authors [12] proposed blends with good fire performance polymers, like phenolic resin, to improve fire resistance of glass fiber reinforced UPE. Nanoparticles were used to favor char retention and, therefore, increase mechanical stability of the structure [13]. Flame retardant coated reinforcements have also been used [14,15] to improve fire resistance of UPE.

Nowadays, unmanaged wastes are causing serious environmental concerns. For that reason, consumption of wastes in the development of new materials is an effective solution to overcome the scarcity of natural resources and to manage the generated wastes. In that sense, many researchers have already used marble powder to produce construction materials like fired clay bricks [16–19] and concrete [20–22], and also different composite materials [23]. During the cutting process, around 20–30% of the marble blocks turns into dust, which is very difficult to stock and, for this reason, constitutes an environmental pollutant. Waste marble powder is composed of calcium and magnesium carbonates and silicates, being calcite ($CaCO_3$) the main component. After firing, new crystalline phases, like wollastonite, gehlenite and anorthite can be formed [17]. Calcium carbonate decomposes in calcium oxide and carbon dioxide at 797.6 °C [18]. TGA (thermogravimetric analysis) studied developed to compare natural marbles from marble residues showed that calcination of calcium carbonate occurs at the same temperature, with little difference in weight loss, regardless of whether it is calcite or limonite. The temperature found was 850 °C and the weight loss was around 43% [24–26]. However UPE is consumed over 600 °C.

Marble presents high values of loss of ignition (LOI), around 41%, and its non-combustion properties have also been reported [23]. Besides, addition of marble dust to clay bricks leads to a reduction on thermal conductivity due to an increase in porosity, which is desired to survive under elevated temperatures [17].

On the other hand, marble is a natural material (metamorphic rock). It is formed when limestone is subjected to heat and pressure. Its main component is calcite ($CaCO_3$), among other minerals [27]. For this reason, marble can be considered as a natural ceramic, since it is a natural material, and it needs to be warmed up in its formation from raw materials.

According to the definition of bio-composite as "a material composed of two or more distinct constituent materials (one being naturally derived) which are combined to yield a new material with improved performance over individual constituent materials" [28], the studied unsaturated polyester and marble material can be considered as a bio-composite, because marble is a natural component regardless of its shape.

Therefore, this research is proposed taking advantage of the properties of UPE and marble dust. Accordingly, the main objective is to obtain a material with good fire resistance and mechanical properties suitable to be used in the habitat industry, for floors or tiles, being an alternative to vinylic or rubber ones. While researches regarding the addition of slag to UPE in order to increase its ablative properties can be found [6], the simultaneous addition of marble wastes and glass fibers to keep the structure under fire and to improve its mechanical properties seems to be clearly innovative. The possible lower performance of UPE compared to phenolic under fire conditions due to char formation can be withdrawn when considering the composite material.

The addition of 50 wt% of marble, used in this paper, is bigger than the amount used in other researches. For

example, Nayak and Satapathy studied the mechanical properties on polyester composites with up to 40 wt% marble dust and evaluating different particle sizes [29], while Nayak et al. studied wear performance of marble composites up to 16 wt% [30].

2. Materials and methods

2.1. Materials and samples preparation

Unsaturated polyester resin (UPE) is a thermoset adhesive obtained by condensation of a diol monomer and an acid monomer in presence of a vinyl monomer [31]. Ferpol 3501 CV2.5 was used in this work. Additionally, this resin needs CH-8 accelerator (cobalt salt in organic acid in aliphatic hydrocarbon solvents) and F-11 catalyst (35% methyl ethyl ketone peroxide, 50% diisobutyl phthalate and dilution solvent), all of them supplied by Feroca S.A. (Madrid, Spain) [32]. The components were mixed in proportion 100:2:2.5 and its density is 1.1 g/cm^3, showing low viscosity. UPE is a thermoset resin; consequently, it does not melt but charry [31]. Charring polymers are required for fire resistance applications, since a carbonaceous residue on the surface is a need for air recirculation to cool the materials placed below [2]. Besides, polyester resins are used to produce polymer concrete due to their high performance, strength, and durability and lower cost [33].

Bio-composites were manufactured by addition of 50 wt.% marble in UPE. Chosen marble powder (Macael 20) has a size particle around 20 μm and the particle diameter at 50% in the cumulative distribution (d50) is 14 μm. It has a density of 2.7 g/cm^3 and its chemical composition (Table 1) was measured by X-ray fluorescence (SPECTRO XEPOS III, Ametek CA, USA). Marble powder was supplied by Triturados Blancos Macael S.A. (Almeria, Spain).

In addition to UPE and UPE/marble materials, samples with 3 wt.% short glass fibers (GF) were prepared. These GF are 6 mm long and their density is 2.58 g/cm^3. Samples with mesh of glass fibers were also prepared, adding 3 wt.% and keeping 50 wt.% of marble. Mesh density is 1.69 g/cm^3 and the mesh size is 3.50 mm. GF and mesh densities were calculated by Archimedes' principle and supplied by Feroca S.A. (Madrid, Spain).

Each mixture was obtained by mechanical mixing at 500 rpm for 5 min. Then the mixture was poured into silicone molds, which have the shape and size according to the specimen requirements for the tests to be carried out. The mesh sheet was also placed manually into silicone molds and cutting according to the test. The samples were cured at room temperature (21−22 °C) for 24 h before testing but all materials were tested one week after they were manufactured and checking their curing grade by T$_g$ (glass transaction

temperature) measurements, thus the presence of curing peak can be detected. T$_g$ was measured by differential scanning calorimetry (DSC) model DSC 820 supplier by Mettler Toledo (Greifensee, Switzerland), for all composites.

From now on, the terminology used for designating the bio-composites will be: +50 *M* for UPE plus marble 50 wt.%; +50 *M*+3 GF for UPE plus marble 50 wt.% and short glass fiber 3 wt.%; and +50 *M*+3 *Mesh* for UPE plus marble 50 wt.% and glass fiber mesh 3 wt.%. This means marble amount is always 50 wt.% and the glass fibers. They will be compared to plain resin (UPE).

2.2. Mechanical properties and wear resistance

2.2.1. Flexural test
Ten samples were tested to calculate flexural strength, according to ASTM D790 standard for three-point flexural test. Microtest universal testing machine (Madrid, Spain) was used at a crosshead speed of 1 mm/min and load cell of 5 kN. Flexural strength and deformation were calculated by Eqs (1) and (2), respectively, where F is the maximum force and L, w and h correspond to width, span length and thickness, respectively.

$$Flexural\ Strength\ (MPa) = (3 \cdot F(N) \cdot L(mm)) \Big/$$
$$\times \left(2 \cdot w\ (mm) \cdot h^2(mm)\right) \tag{1}$$

$$Deformation\ (\%) = \left((6 \cdot \delta\ (mm) \cdot w\ (mm)) / (L^2(mm))\right) \cdot 100 \tag{2}$$

2.2.2. Charpy impact test
Charpy impact tests were carried out with a pendulum impact testing machine CEAST 9050 Instron (Barcelona, Spain), according to ASTM E23 standard. The absorbed energy on Charpy impact test (E) was obtained by Eq. (3), with the following parameters: mass of the hammer (W), gravitation acceleration (g = 9.80655 m/s^2), length (R), angle at the end of the swing (β), angle of fall (α) and energy loss (L). To be able to compare among the different materials, resilience was calculated according to Eq. (4). Ten samples of each material were tested.

$$Absorbed\ Energy\ (kJ) = W \cdot g \cdot R(\cos\beta - \cos\alpha) - L(mm)) \tag{3}$$

$$Resilience = (Absorbed\ Energy\ (kJ)) / (So\ (m^2)) \tag{4}$$

2.2.3. Compression test
The compression strength tests of prismatic specimens were performed in a Microtest universal testing machine (Madrid, Spain) according to ASTM 695-15 standard. Five samples of each material were molded with a size of 24.6 mm × 12.3 mm x 12.3 mm. The tests were carried out at 1.0 mm min^{-1} with a 10 kN load cell and temperature around 22 °C. Compression strength was obtained by quotient of maximum force (N) and area, in this case 151.29 mm^2.

2.2.4. Wear test
Dry sliding wear tests were carried out at room temperature using a pin-on-disk tribometer (Microtest, Madrid, Spain). In this test, a stationary specimen (pin) with a defined normal

Table 1 − Chemical composition of Macael 20 marble powder.

Chemical composition (%)	CaCO$_3$	MgCO$_3$	Fe$_2$O$_3$	Al$_2$O$_3$	SiO$_2$
	>98.0	<1.5	<0.2	<0.1	<0.2

force is pressed against the surface of another specimen placed on the rotary disk. The normal force is applied over the pin or ball by means of a set of dead weights between 0 N and 60 N (in this case, 15 N was applied). This way of application allows a stable force during the test. A 6 mm diameter alumina ball was used for the pin. The test conditions were 120 rpm, relative humidity below 30% and friction radius of 8 mm. The sliding distance was 1000 m.

Wear was evaluated using Archard equation (Eq.n (5)). To calculate wear and friction coefficient, ASTM G99-05 standard was used. Wear resistance was calculated by volume loss according to weight loss and density of the samples, which was measured by Archimedes' principle, using an alcohol pycnometer and a weighing scale with 5 digits (Mettler Toledo GmbH, Greifensee, Switzerland).

In these tests, no significant pin wear was assumed, and the wear debris was not removed from track, as its importance has been demonstrated for fretting wear models [34].

$$Wear = (Weight\ loss\ /\ density)/(Load \cdot Sliding\ distance) \quad (5)$$

To determine the wear mechanism, wear tracks after testing were observed with a DSX500 opto-digital microscope (OM) supplied by Olympus Corporation (Tokyo, Japan). Besides, scanning electron microscopy (SEM), using a Philips X-30 model (Philips Electronic Instruments, Mahwah, NJ, USA), was used to study the fracture surface of flexural and impact tested samples, together with wear tracks. The samples were coated with gold before SEM study.

2.3.   Fire resistance

Three sheets of 100 mm × 100 mm with a thickness of 3.5 mm were manufactured for each bio-composite to carry out fire tests. The tests consist in a flame at 900 °C (measured with a thermocouple), obtained from Bunsen burner, which was fueled by propane gas and placed in front on the sample. The reducing zone of the flame was in contact with the material during the test (Fig. 1A). Temperature was measured opposite to fire test side of the samples with a FLIR infrared camera model E95 (FLIR Networked Systems S.L., Madrid, Spain), according to Fig. 1B. The thermographs were taken every 20 s, being possible to follow the fire test with the 3D images. Temperatures were exported from images to plot time evolution of temperature.

2.4.   Thermal conductivity

Thermal conductivity was determined by differential scanning calorimetry (DSC), model 822 equipment (Mettler Toledo, Greifensee, Switzerland). As purge gas, 80 mL/min nitrogen was used. The thermal cycle was from 20 to 38 °C at 0.5 °C/min [35]. The method is based on the stationary regime; it involves placing a pure metal (e.g., indium or gallium) in a crucible on the material to be measured (without crucible), and both placed directly on the DSC sensor [36].

The material was prepared in cylinders (3 mm diameter) with an approximate height of 2 mm. Before performing the DSC measurement, area and volume of cylindrical pieces of material were measured. All measurements were repeated five times.

3.   Results and discussion

3.1.   Mechanical properties

3.1.1.   Flexural strength
Ten samples of each material were tested to measure flexural strength and deformation (Eqs. (1) and (2)). Besides, flexural modulus was calculated for flexural strength at 30 MPa, thus all materials can be compared. Fig. 2 shows the data of flexural tests.

A provides information on flexural strength (Fig. 2A): for UPE, it is 40 MPa and bio-composite with marble increases until 55 MPa. When short glass fibers were added, it increases 8 MPa more, thus the fiber improves the flexural strength of
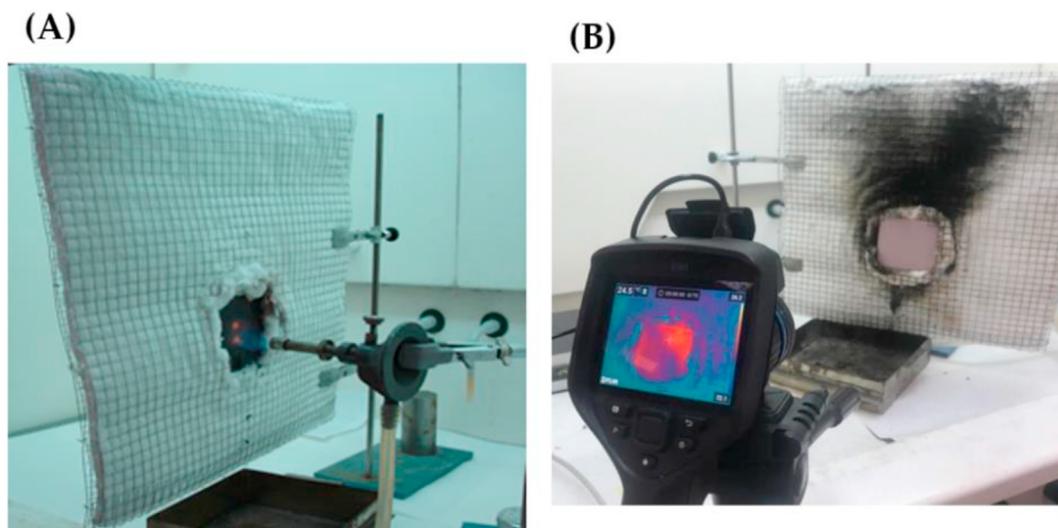

Fig. 1 − Fire test setup (A) in front of the sample, and (B) infrared camera opposite to fire test side of the sample.
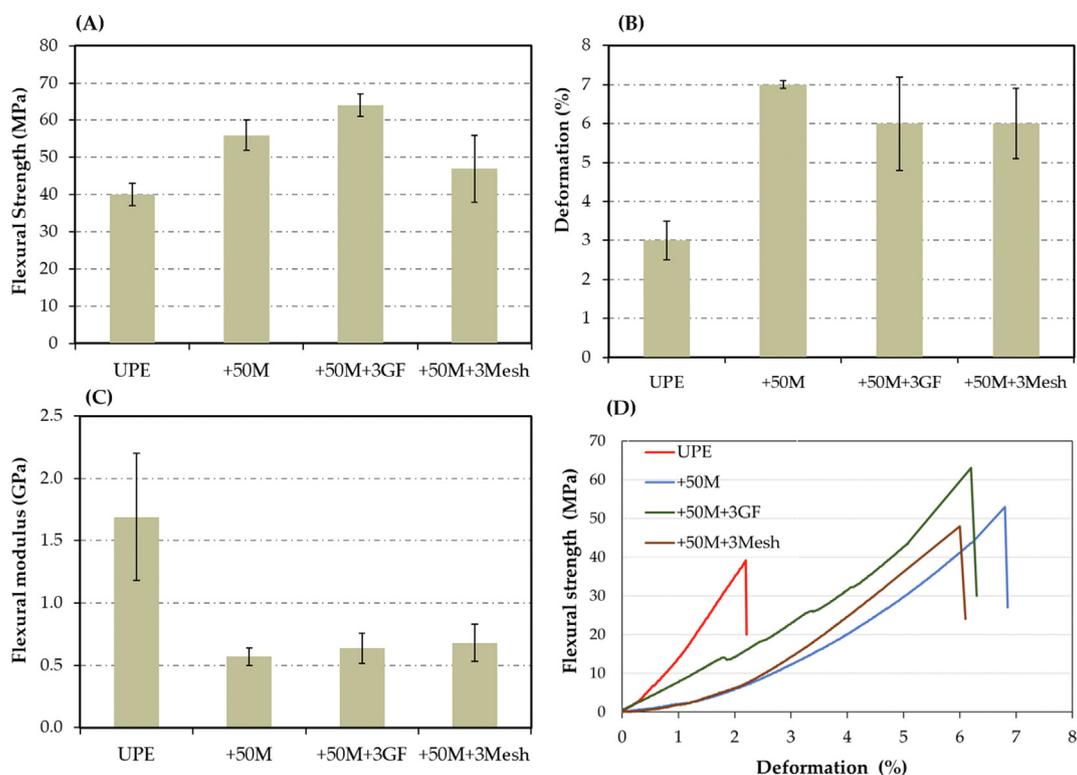
Fig. 2 — (A) Flexural strength (B) deformation (C) flexural modulus at 30 MPa for the four materials and (D) average curves of flexural tests.

the bio-composite. Previous studies [37] with SiC and short glass fiber in UPE matrix showed that the addition of particles increased flexural strength (up to 55 MPa), similarly to marble particles. When short glass fibers are added, the increase found with marble was not found with SiC. However, when mesh is introduced in the material, flexural strength decreases and data dispersion increases because mesh fiber is not always located in the same position. Tests of bio-composites with mesh were stopped before total breakage since the mesh did not break. These flexural strength values are higher than the values found by Benzannache et al. [38] for polymer concrete with marble and sand in percentage of 86 wt %, being 35 MPa the highest value for composite with 43 wt% of sand and 43 wt% of marble waste.

Fig. 2B shows how deformation also increases for the bio-composites. This effect may be attributed to less cross-linking of UPE chains that allows greater slipping since the lower half of flexural samples is subjected to tensile loads and the upper half to compression loads, when the direction of force is considered. T_g values for all composites (100 ± 2 °C) are smaller than that of neat UPE (140 ± 2 °C), suggesting that marble particles hinder crosslinking. However, full curing took place in all materials, as there was no curing peak after curing for 24 h. This decrease in crosslinking leads to higher deformation compared to neat UPE, although composites still present rigid behavior. Error bars are higher when there are fibers since the test depends on fiber position, and flexural samples might have different number of filaments in the case of composite with 50M+3 mesh due to manufacturing process (section 2.1).

Flexural modulus (Fig. 2C) decreases for bio-composites. This effect is related to a decrease in the crosslinking among polyester chains due to the presence of marble and GF. GF effect is not significant in terms of flexural modulus; thus, the bio-composites have similar modulus, about 0.6 GPa, being UPE modulus around 1.6 GPa. These values agree with a rigid material. The bio-composites obtained in this work have higher flexural strength and strain than a polymer concrete manufactured with marble, quartz sand and glass fibers [39]

Fig. 2D shows the curves of flexural tests for the different materials. Curves represent the average of the 5 tests carried out. Improvements in both strength and deformation can be appreciated comparing the bio-composite materials with the matrix. High flexural strength and deformation suggests that the toughness of the bio-composite has increased, as it is possible to verify in the increase of the area under the curve for bio-composites (Fig. 2D). As results of the increase in deformation, flexural modulus decreases when marble is added. Therefore, the rigidity of the material decreases.

The bio-composites have higher flexural strength and deformation than plain UPE, which is an indicator of a good join between marble and UPE; this can also been observed in Fig. 3A, since polyester drops wet marble surface with very small contact angles. This joint can stop the crack growth and the strength can increase (Fig. 2A). Randomly distributed short fibers can improve strength if they coincide in the break line. However, samples with mesh do not break although part of the UPE+50M breaks, leaving the parts joined by the mesh. The marble distribution is homogeneous, as it can see in
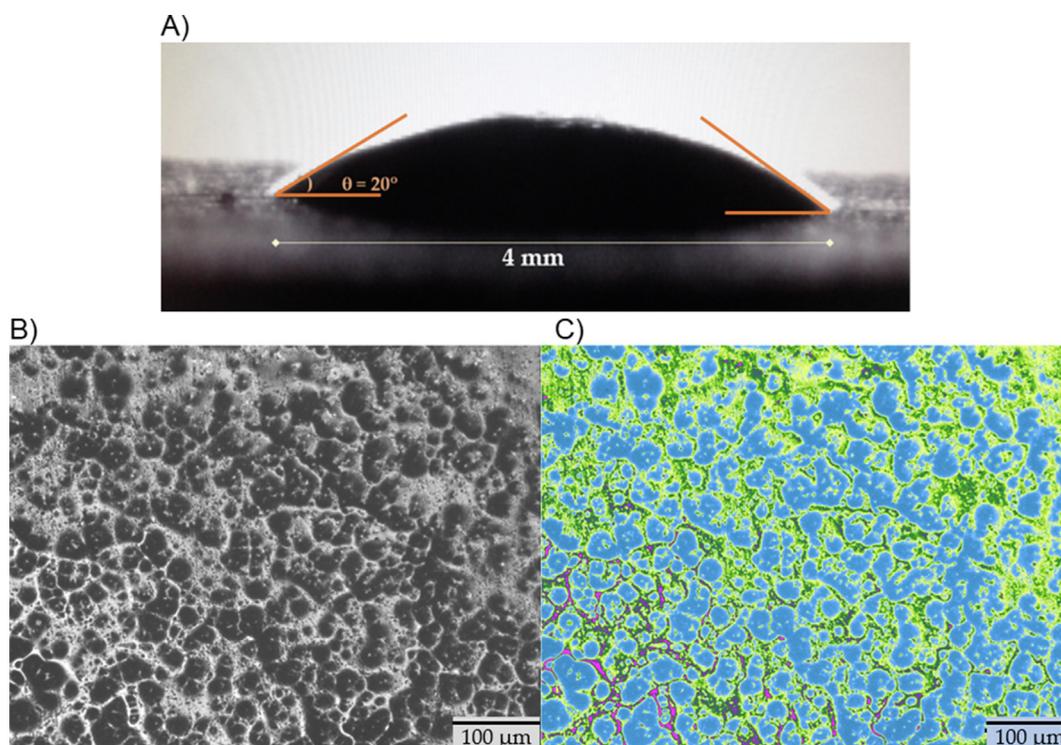
Fig. 3 − A) Macrograph of a polyester drop on marble, B) Optical micrograph of bio-composite +50M and C) Optical micrograph with color filter (blue − marble particles and green − UPE).

Fig. 3B and C. This distribution also improves the properties of the bio-composites, distributing the efforts in all directions.

Fig. 4 shows the fracture surfaces of the flexion tested specimens. When plain UPE is observed (Fig. 4), the fracture surface presents flat planes typical of a brittle polymer; this explains the low deformation (Fig. 2B) and high flexural modulus (Fig. 2C). However, for the sample with 50 wt.% marble (Fig. 4), marble particles are broken and fracture surface reveals flat planes along with cracks reaching the particle (red circle in Fig. 4); in this micrographic interphase can also be analyzed and good adhesion between marble and the matrix is found. Consequently, this material has higher flexural strength, although the matrix is brittle like plain resin. Specimens with short GF (Fig. 4) present broken fibers on the fracture surface that can slightly increase flexural strength (Fig. 2A). Although GF slightly stiff the material (deformation decreases and flexural modulus increases (Fig. 2B and C), these changes are slight since the percentage of glass fibers is little. Moreover, the error bars are bigger than for other materials due to the random distribution of the short glass fibers. Specimens with mesh (Fig. 4) have a similar behavior, although the fracture surface shows the mesh imprint and it seems that the bond between mesh and resin is not complete, which can cause a slight decrease in strength (Fig. 2A).

3.1.2. Impact test

Fig. 5A shows the resilience values calculated from impact test according to Eq. (4). Impact test provides high energy absorption for composite with mesh, showing 96 kJ/m^2

compared to 7 kJ/m2 for short GF composite. These values are considerably higher than those of marble composite or UPE, being 2 kJ/m2 and 1 kJ/m2 of, respectively. Fibers have a positive effect on energy absorption and the addition of GF improves resiliency, in general. Fibers withstand the impact, having more resistance when fiber content is higher in the impact area. Error bars are affected by the placement of the fibers in the sample. The mesh does not break, remaining the parts attached, as it can be seen in Fig. 5B.

The fracture surfaces of UPE exhibited characteristic typical of brittle failure, with a smooth and glossy aspect, according to Fig. 6. The fracture surface changes significantly when marble was added. Particles absorb energy from the impact and marble particles break by cleavage (Figs. 6 and 7). When adding marble, a slight deformation is observed compared to UPE. When fibers are present, they need to be pulled up (Fig. 6) and broken, but samples do not completely break, thus resilience increases. As previously seen in Fig. 2, resilience values show that the addition of marble and, in a greater extent, the glass fiber mesh, increases toughness of UPE. High resilience agrees on increase in the toughness of the bio-composite and it is in agreement with what was found in the flexural behavior, although the impact tests are carried out at a higher speed than the bending tests. Fig. 7 also shows a good adhesion between marble and polyester matrix.

3.1.3. Compression test

Fig. 8 and Table 2 show the representative compression curves for all materials and the average compression strength and

Table 2 – Average compression strength and strain at maximum load.

Material	Compression strength (MPa)	Strain at maximum load (mm/mm)
UPE	90.0 ± 2.5	0.13 ± 0.03
+50M	76.5 ± 6.9	0.09 ± 0.01
+50M + 3GF	90.5 ± 3.1	0.04 ± 0.01
+50M + 3mesh	86.6 ± 5.8	0.05 ± 0.01

failure strain of the five tests respectively. UPE presents high compression strength being the material with highest deformation ability. When 50% of marble is added, the maximum compression load decreases around 15% and the failure strain decreases too. However, when glass fibers are added to the bio-composite, strength rises to values similar to UPE although less strain is measured. The values obtained for the UPE are similar to those that could be found in the literature [4], where Barros et al. report similar value for UPE while limestone addition also decreases compression strength is lower as the percentage of UPE decreases. This is due to high compressibility of UPE, when UPE amount decreases, the compression strength also does [4]. If instead of microparticles, nanoclay is added, then the compressive strength increases [40]. Glass fibers reduce the negative effect of marble on compressibility, being the strength similar to UPE, since the fibers provide resistance to crack propagation and crack opening [41].

Another remarkable difference takes place in failure. UPE is totally squashed with a great deformation at the end of test, whereas the composites collapse and crack with less strain. For this reason, the UPE curve drops at the end when the material is already squashed.

3.1.4. Wear resistance

Dry sliding wear tests provide the friction coefficient vs. sliding distance (Fig. 9A). The average of the steady-state part of these curves is the friction coefficient used to compare the different materials of this study. In these materials, the curves are stable from initial sliding, thus, average line is a straight line and on the y axis it is possible to read friction coefficient as it is shown in Fig. 9A (red line). Fluctuations between 0.4 and 0.6 are due to the shedding of marble or resin particles, which produces abrasion between the two sliding surfaces. The rise in the coefficient of friction for bio-composites (Fig. 9B) could be due to the abrasive marble particles which cause third-body abrasion when present at the sliding interface. This third body could protect the matrix and, consequently, wear decreases, as Fig. 9C shows. Bhatia et al. [42] observed this effect with glass microspheres and boron carbide reinforcing an epoxy resin. When, there is good adhesion between matrix and particles [43], hard particles in composites usually increase friction coefficient and improve wear resistance [44–46]. This is due to the marble particles are doing third body effect but at the same time they are coated with polyester that favors adhesion on the polyester itself. In this study, this trend can be observed for every bio-composite, except for 50M+3 GF, in which wear is higher due to the
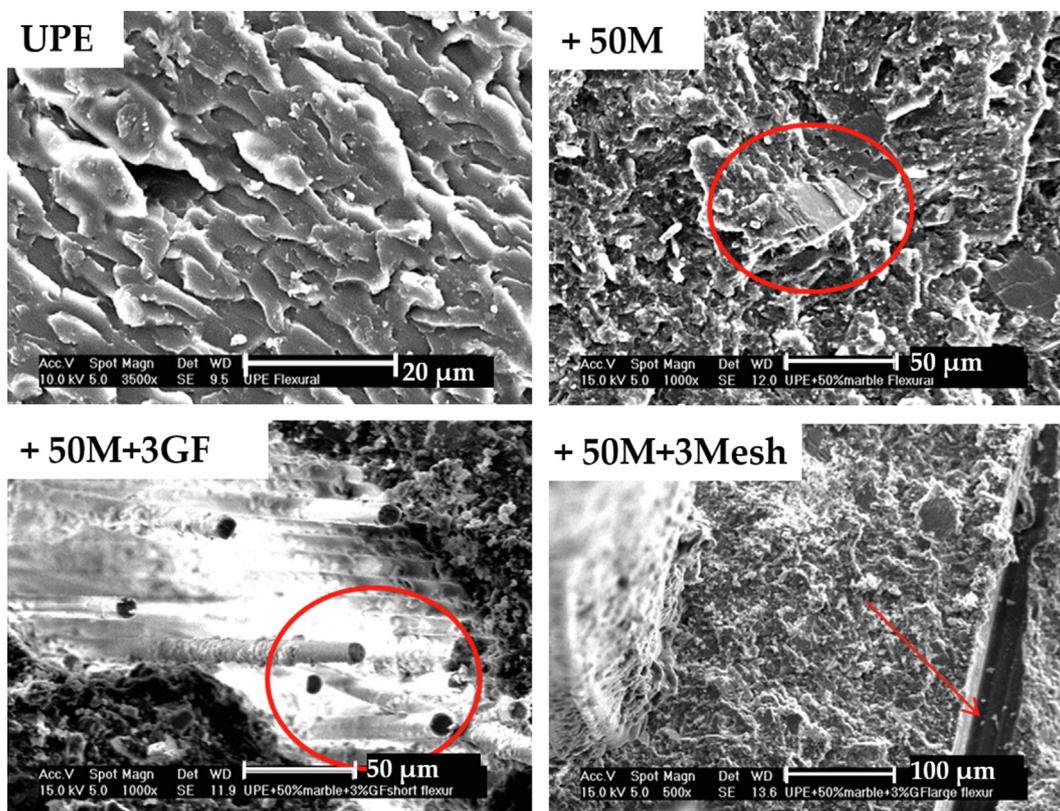

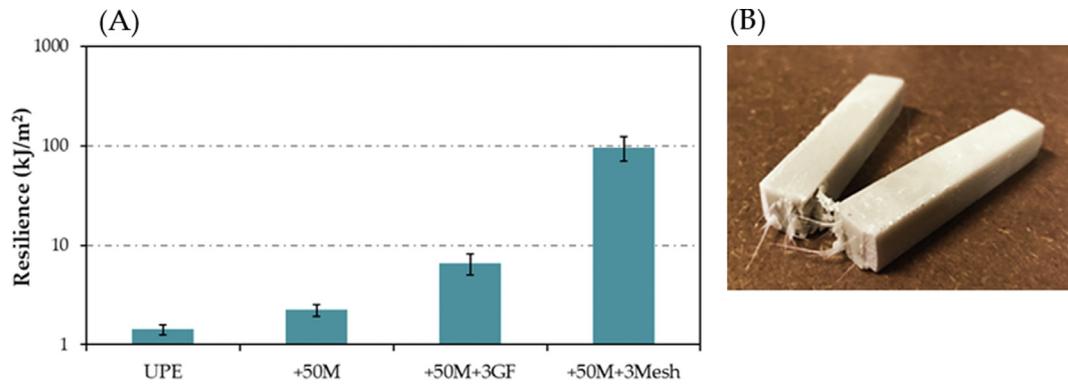**Fig. 4 – Micrographs of flexure specimen fractures.**

Fig. 5 − (A) Results of resilience obtained from impact test and (B) failure of sample with mesh.

presence of short glass fiber that does not allow the worn particles to adhere on its surface.

Worn surface morphology was studied by optical microscopy (Fig. 10) and SEM (Fig. 11), to understand the wear mechanism.

The four 3D images (Fig. 10) show wear tracks of UPE and its bio-composites. UPE has the widest track, although it is not very deep and it presents fewer deposits than the wear tracks of bio-composites. Bio-composite with marble presents a shallow and less wide track than UPE, with adhesion (deposits) at the edges, whereas the bio-composite with marble and short GF has a deeper and slightly wider track, with little build-up at the edges. The track of the bio-composite with marble and mesh presents a shallow track with a narrow central zone of abrasive wear and more build-up of material at the edges, predominantly adhesive wear and a track more similar to composite with marble. The most important process to remove material in dry sliding wear is abrasive wear, which can proceed through different wear mechanisms, among others, matrix wear, filler sliding wear or interfacial debonding [47]. Abrasive wear is due to hard particles or hard protuberances on the track, forming grooves on the surface. In this study, hard particles are present and they have a double effect: on the one hand, they increase the friction coefficient and, on the other hand, they protect the matrix, improving wear resistance [48]. As Fig. 10 shows, short GF have a negative
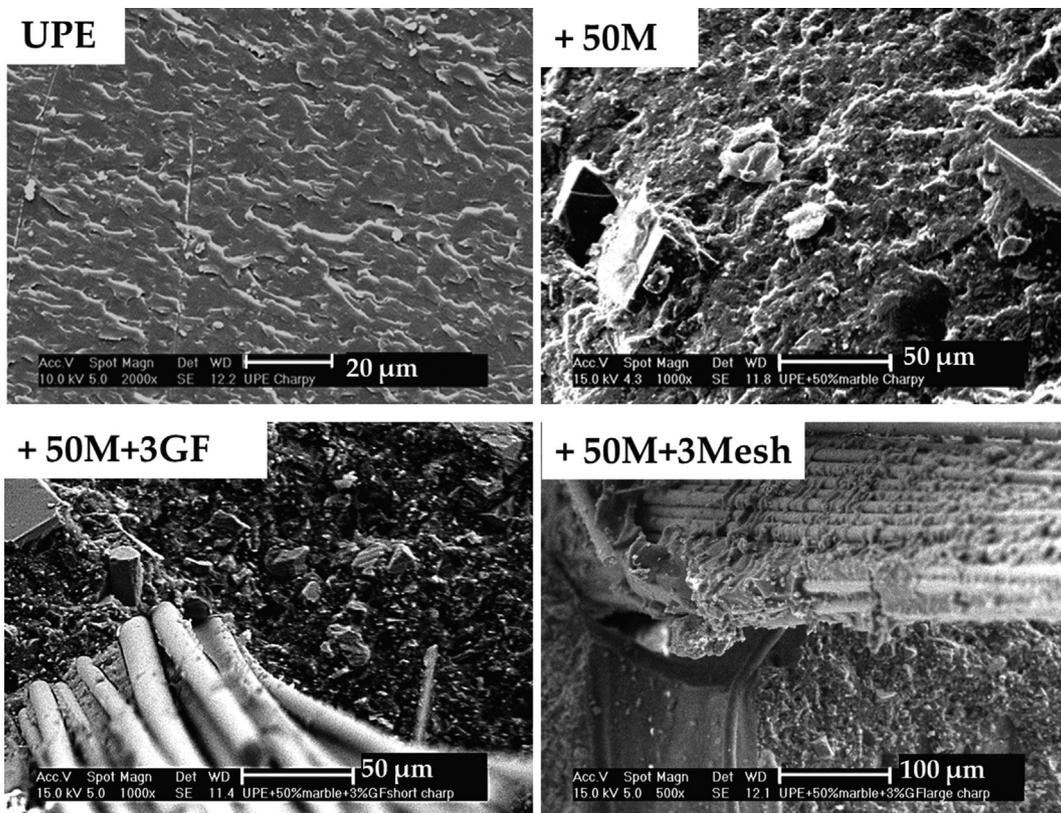

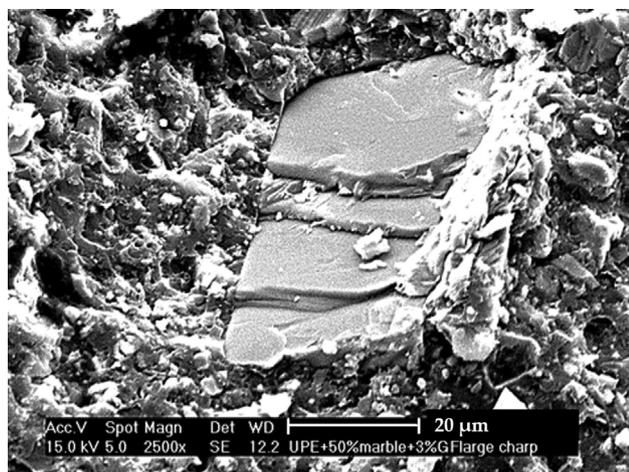**Fig. 6 − Micrographs of impact test specimen fractures.**

Fig. 7 — Fracture surface detail of marble particles on impact test sample of 50M + 3GF.

effect since they can come off the track (implying weight loss, hence more wear),- they also can suffer fiber sliding wear and, consequently, generate a deeper track. Furthermore, +50M+3 GF bio-composite does not allow the marble particles adhesion on it (Fig. 11), thus it presents worse wear behavior, although better than plain UPE.

Wear behavior of UPE is considerably worse than polypropylene (PP), since the former is a thermoset and PP is a thermoplastic. However, when marble is added to UPE and silicon carbide to PP, the wear value is the same for both of them [49]. Therefore, the addition of marble improves not only the matrix, but its behavior can be similar to that of a thermoplastic composite.

SEM micrographs (Fig. 11) clearly show those features. The predominant wear mechanism is abrasive. UPE (Fig. 11) shows abrasive wear on the sliding wear track and some re-adhesion in another area, without particles or debris on the surface. This indicates that some resin particles are completely removed and others bond again. Conversely, bio-composite wear tracks show wear debris (hard particles) and grooves typical of sliding wear, with hard protuberances that can cause the oscillation of friction coefficient (Fig. 9A), but there is also re-bonded debris (worn material) on the edges of grooves and tracks.

3.2. Fire resistance

Vertical tests were carried out to study fire resistance. UPE degradation takes place from 200 °C to 600 °C, according to Tibiletti et al. [50], when the reaction is carried out in air. Loss of water by dehydration occurs around 250 °C. This step is followed by the chain scission of polystyrene and polyester fragments, and carbonaceous char is obtained, that is further degraded around 600 °C. As flame temperature is 900 °C during test, UPE completely transforms into char. Black area in Fig. 12 shows completely degraded and ruined UPE after test. This occurs for UPE and bio-composites without mesh.

Bio-composites perform in a different manner, due to the presence of marble. Fig. 13 shows a sequence of

thermographs. For each image, the temperature on the upper left corner (i.e., 327 °C in the first one) corresponds to temperature in the cross-marked point (center of each image), and that on the upper right corner (380 °C for the same instant) is the maximum temperature in the sample (brightest and whitest area). Initially, both temperatures increase, although the maximum measured temperature (on the right) does faster, reaching a maximum of 603 °C (marked with the red arrow) and then begins to decrease. The instant for this maximum does not coincide with that on the center of the tested area, showing a maximum of 523 °C (marked with the red arrow), decreasing from that instant. It is noticeable that this behavior occurs in the 3 bio-composites, although maximum temperature values change.

Looking to the front side of fire-tested materials, the brown and white areas (Fig. 14A) correspond to areas where the UPE degradation and calcium carbonate reaction take place at the same time, since the temperature is higher than 800 °C (as flame presents 900 °C and its temperature increases very fast). Therefore, there is UPE degradation in brown areas and calcium oxide in white areas after 10 min of fire test. Around the bright and white maximum temperature spot (Fig. 14B), there is a yellow area that indicates $CaCO_3$ decomposition, and corresponds, macroscopically, with presence of calcium oxide (Fig. 14A). Although water loss and chain scission of UPE is occurring, no further charring takes place. The main reason is the presence of marble particles. When temperature on the surface surpasses 800 °C, calcium carbonate of marble particles starts to transform into CaO. This transformation of calcium carbonate is an endothermic reaction, absorbing heat during the process. According to the reaction, one mole of calcium carbonate needs 178.3 kJ/mol to transform into one mole of calcium oxide and one mole of carbon dioxide. Samples used in this study contain 44 g of marble; hence they are able to absorb 77 kJ.

According to Fig. 13 (opposite to fire test side), maximum temperatures above 600 °C appear on the surface, but majority of the surface does not reach that temperature. There is a difference of roughly 200 °C between both sides, related to thermal conductivity. Although marble slightly increases thermal conductivity of polymer matrix composites [51], it remains very low, and this is the second reason so that the
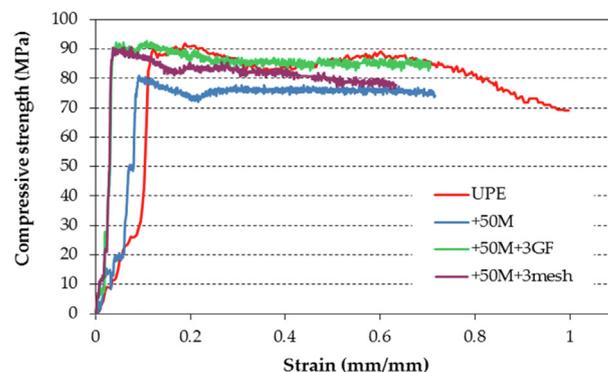

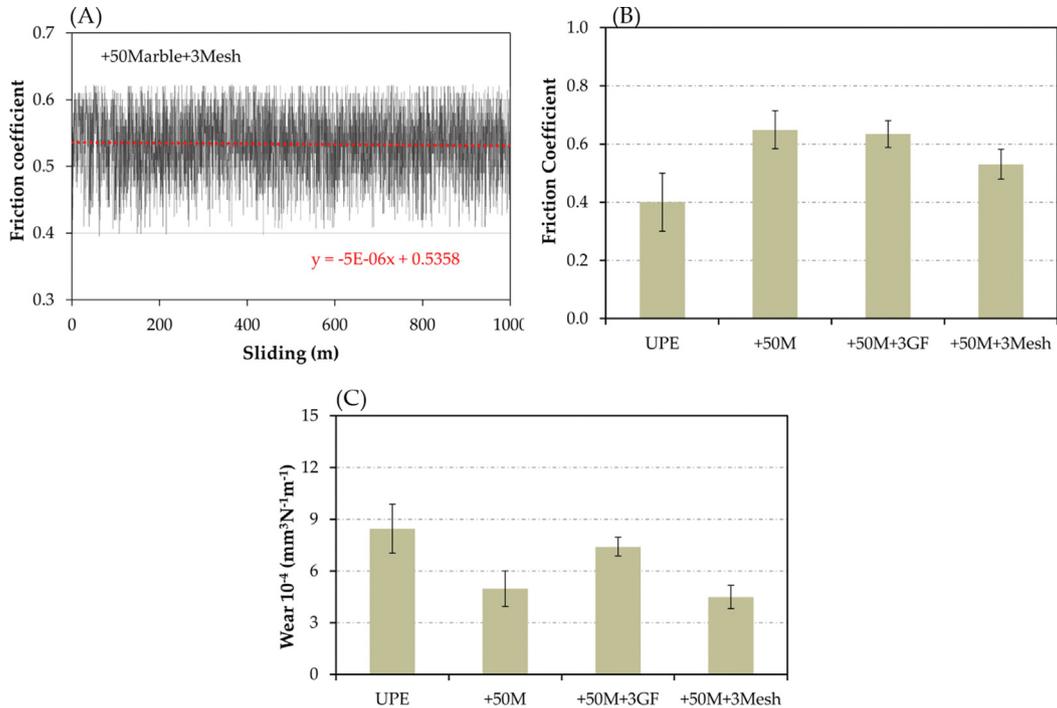**Fig. 8 — Representative compression curves for all materials.**

Fig. 9 − (A) Representative friction coefficient evolution vs sliding curve of bio-composite with 3% of mesh (B) Friction coefficients and (C) wear resistance for bio-composites and UPE matrix.

UPE does not char so quickly. In this case, thermal conductivity of marble bio-composite is 0.308 W/m·K, compared to 0.154 W/m·K of UPE. As it was explained in Section 2.4, thermal conductivity was measured by DSC following a method previously used by the authors [52].

The curves of Fig. 15 show maximum temperature variation of composites during fire test, showing the degradation phenomena. The sharp increase of temperature (from 350 °C) relates to UPE degradation through chain scission. When temperature surpasses 600 °C, marble present in bio-composites starts to transform. Its endothermic combustion reaction consumes heat, reducing the temperature as heat is conducted in the plate (Fig. 13 shows the increase of temperature in the rest of the plate). Temperature decreases and it
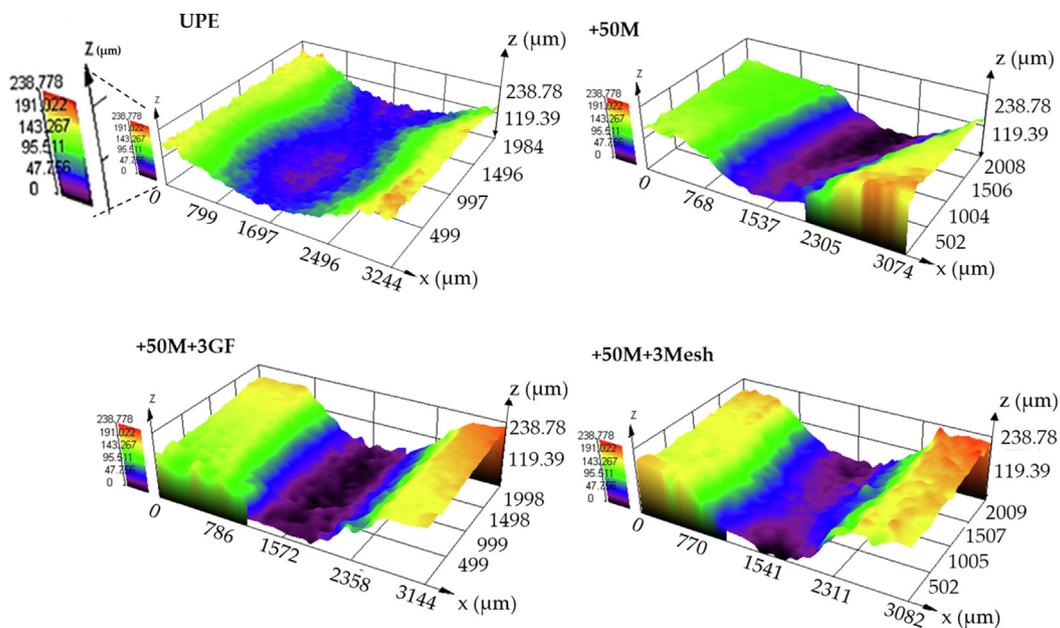

Fig. 10 − 3D images by optical microscopic for UPE matrix and bio-composites. Z-axis is the same for all 3D images; it is enlarged on the UPE image.
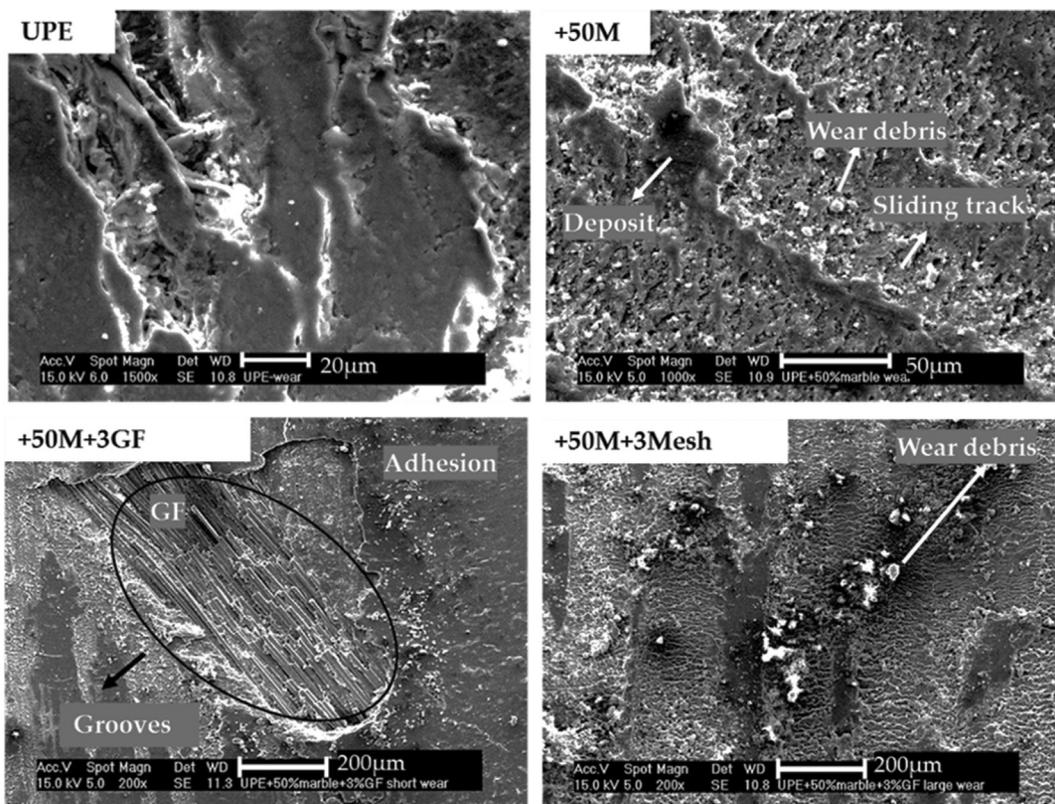
Fig. 11 – Wear track micrographs by SEM for the UPE and bio-composites.

Fig. 12 – Macrograph of carbonized wastes of UPE after fire test of any sample (Picture after a fire test for 30 min of +50M + 3GF bio-composite).

stabilizes around 520 °C for a long time. Moreover, it is remarkable that the CO_2 released is able to go out the flame once the burner is turned off. All the tests were carried out for 20 min, when Bunsen burner was turned off and the flame went out alone.

Although an electrical burner was not used in this work, bio-composite sheets were narrower than 5 mm and they can be considered as flexible materials. They do not drip and there is no ignition for more than 5 s after removing the flame. Therefore, according to UNE 23727:1990 standard, these bio-composites can be classified as M1. Besides, as one of the sides does not ignite, its flammability index would be infinite. However, more, different fire tests would be required before final application of these materials can be claimed.

UPE presents some limitations due to its brittleness that makes it unsuitable to be used under impact. As a polymer, its fire resistance is also limited. With marble addition, these two factors are improved and its applications are broader. The main advantage of the developed bio-composite, compared to currently used rubber and vinyl, is its fire resistance together with its lower cost. Furthermore, as some materials like micro-cements, it could be mixed and applied during the construction; therefore viscosity is not a limiting factor.
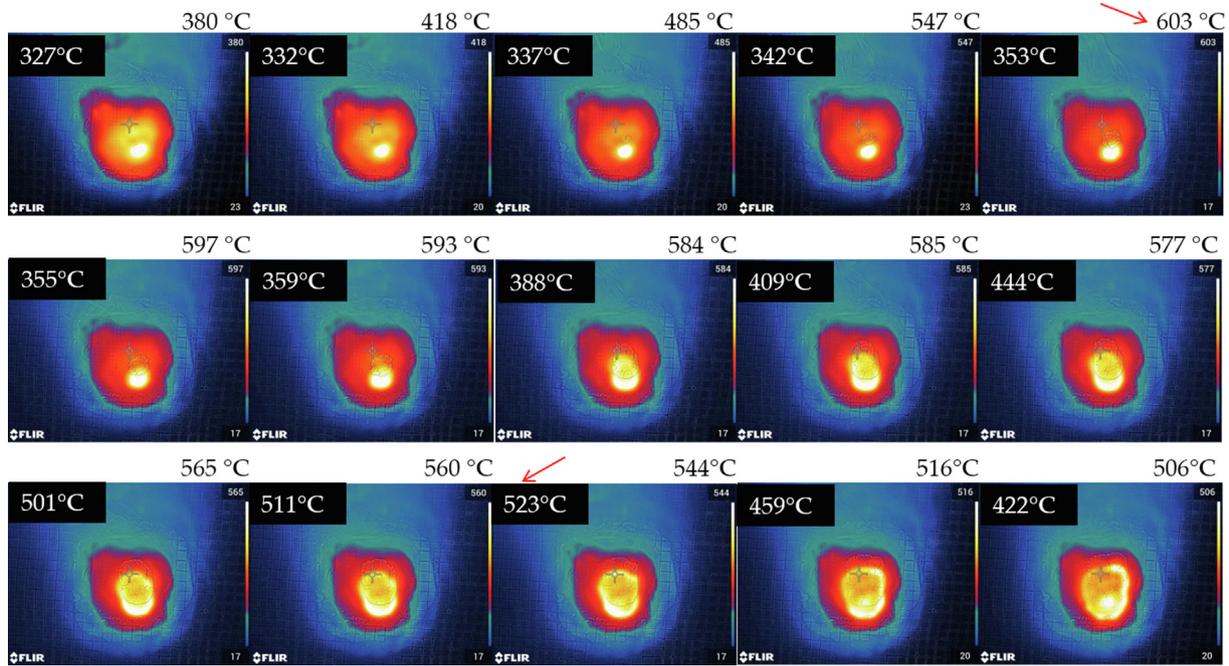
Fig. 13 — Sequence of thermographs corresponding to the opposite to fire test side of +50M sample, during fire test.
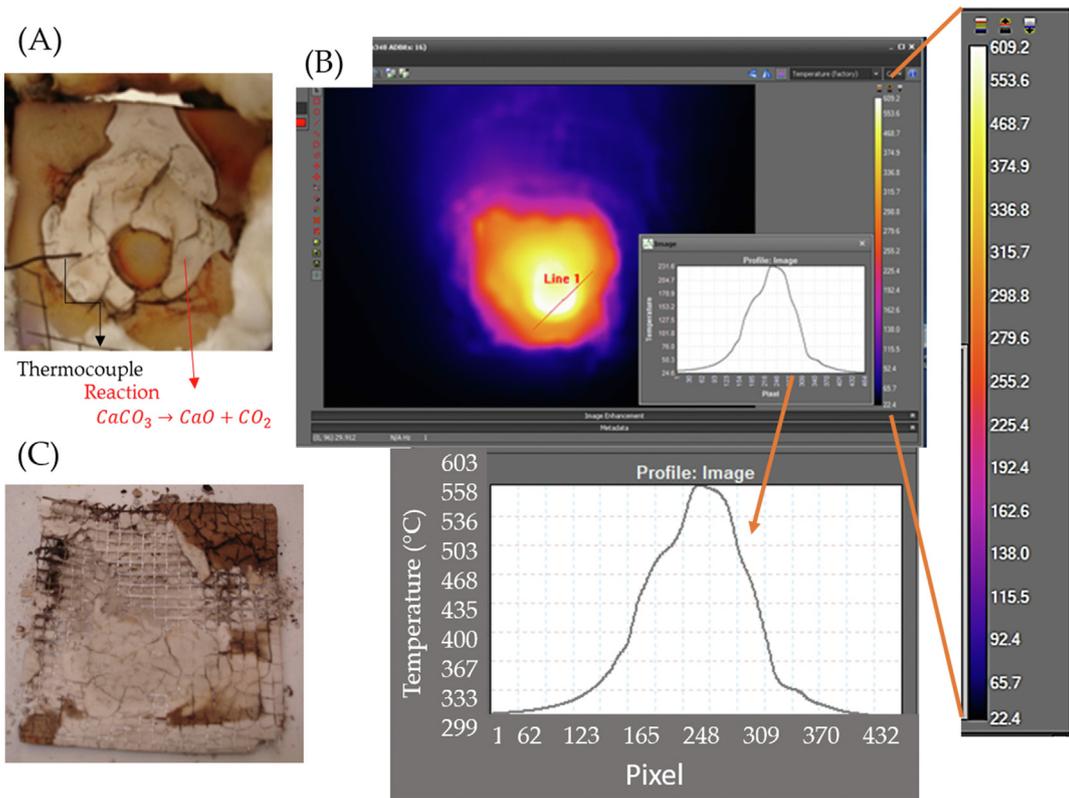

Fig. 14 — Fire test (A) picture taken during test at 10 min, in front fire test side (B) temperature profile taken by infrared camera opposite to fire test side (C) picture after a fire test for 30 min of bio-composite +50M + 3 Mesh.
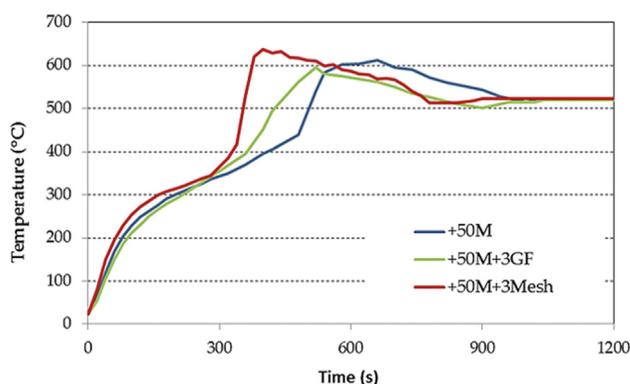
Fig. 15 – Temperature versus time curves for all bio-composites during the fire test, measured at the opposite to fire test side.

4. Conclusions

The main objective of this work was achieved: manufacturing and testing a material with properties on demand and good fire resistance, made of unsaturated polyester, marble and glass fibers.

Regarding the influence of marble and glass fibers on mechanical and wear properties of polyester, following conclusions can be drawn:

- Marble leads to a change on impact and wear properties, increasing both resilience and wear resistance. Wear resistance rises due to third-body effect of the marble, promoting high friction coefficients. However, compression strength decreases around 15%.
- With the addition of short glass fibers, resilience is increased, but wear properties decrease since the loss of fibers is associated with higher weight loss. If the short fibers are replaced by mesh, both resilience and wear resistance increase. Additionally, compression strengths keep the same values as the UPE, but all marble samples collapse, whereas UPE squash to the compression.

Fire resistance is not modified by glass fiber addition, although the mesh maintains the integrity of the sample when the resin burns, and the flame goes out; the sample collapses when no fibers or no fibers are present in the material.

The reaction of $CaCO_3$ takes place releasing CO_2, which is responsible for the high fire resistance and the flame extinction. Furthermore, a temperature decrease and stabilization is produced, during transformation, once UPE degradation finishes.

According to these results any of these composites would be able to be used in the habitat industry, since they may be classified as M1, they have good impact resistance and good wear properties. Specially, the choice of 50M+3 GF would be valid for floors, while 50M+3 mesh would be better for walls since it maintains the structure for longer times.

Author contributions

Conceptualization, J.A. and M.-A.M.; methodology, J.A. and M-A.M.; validation, J.A., M-A.M. and S.L.d.A.; formal analysis, J.A., M.-A.M and S.L.d.A.; investigation, J.A. and M-A.M.; resources, F.V. and M.-A.M.; writing—original draft preparation, J.A.; S.L.d.A., and E.P.; writing—review and editing, J.A, S.L.d.A., E.P., J-C.d.R., F.V.; visualization, J.A. and M-A.M.; supervision, J-C.d.R.; project administration, F.V.; funding acquisition, F.V. All authors have read and agreed to the published version of the manuscript.

Funding

Declaration of Competing Interest

The authors declare that they have no known competing financial interests or personal relationships that could have appeared to influence the work reported in this paper.

Acknowledgments

REFERENCES

[1] Pulci G, Paglia L, Genova V, Bartuli C, Valente T, Marra F. Low density ablative materials modified by nanoparticles addition: manufacturing and characterization. Compososite Part A Appl. Sci. Manuf. 2018;109:330–7. https://doi.org/10.1016/j.compositesa.2018.03.025.

[2] Natali M, Kenny JM, Torre L. Science and technology of polymeric ablative materials for thermal protection systems and propulsion devices: a review. Prog Mater Sci 2016;84:192–275. https://doi.org/10.1016/j.pmatsci.2016.08.003.

[3] Venkatapathy E, Laub B, Hartman GJ, Arnold JO, Wright MJ, Allen GA. Thermal protection system development, testing, and qualification for atmospheric probes and sample return missions. Examples for Saturn, Titan and Stardust-type sample return. Adv Space Res 2009;44:138–50. https://doi.org/10.1016/j.asr.2008.12.023.

[4] Barros MM, Ferreira Leão de Oliveira M, Ribeiro RCC, Cruz Bastos D, Gomes de Oliveira M. Ecological bricks from dimension stone waste and polyester resin. Construct Build Mater 2020;232:117252. https://doi.org/10.1016/j.conbuildmat.2019.117252.

[5] Morales Arias JP, Escobar MM, Bernal C, Vázquez A. Aging in water and in an alkaline medium of unsaturated polyester and epoxy resins: experimental study and modeling. Adv Polym Technol 2016;201:21684. https://doi.org/10.1002/adv.21684.

[6] Robayo-Salazar R, Portocarrero-Hermann J, Díaz-Padrón U, Patiño-Castrillón O. Polymeric ablative composite materials and their application in the manufacture of aerospace propulsion components. Revista Facultad de Ingeniería, Universidad de Antioquia. 2020;29:e10662. https://doi.org/10.19053/01211129.v29.n54.2020.10662.

[7] Zhao D, Wang J, Wang XL, Wang YZ. Highly thermostable and durably flame-retardant unsaturated polyester modified by a novel polymeric flame retardant containing Schiff base and spirocyclic structures. Chem Eng J 2018;344:419−30. https://doi.org/10.1016/j.cej.2018.03.102.

[8] Lu SL, Hamerton I. Recent developments in the chemistry of halogen-free flame retardant polymers. Prog Mater Sci 2002;27:1661−712. https://doi.org/10.1055/s-2002-33635.

[9] Dai K, Song L, Yuen RKK, Jiang S, Pan H, Hu Y. Enhanced properties of the incorporation of a novel reactive phosphorus- and sulfur-containing flame-retardant monomer into unsaturated polyester resin. Ind Eng Chem Res 2012;51:15918−26. https://doi.org/10.1021/ie302106w.

[10] Pan LL, Li GY, Su YC, Lian JS. Fire retardant mechanism analysis between ammonium polyphosphate and triphenyl phosphate in unsaturated polyester resin. Polym Degrad Stabil 2012;97:1801−6. https://doi.org/10.1016/j.polymdegradstab.2012.06.002.

[11] Gao M, Wang H, Wang Y, Shen T, Wu W. Flame retardancy and mechanical properties of a novel intumescent flame-retardant unsaturated polyester. J Vinyl Addit Technol 2014;22:350−5. https://doi.org/10.1002/vnl.

[12] Kandola BK, Krishnan L, Ebdon JR, Myler P. Structure-property relationships in structural glass fibre reinforced composites from unsaturated polyester and inherently fire retardant phenolic resin matrix blends. Compos B Eng 2020;182:107607. https://doi.org/10.1016/j.compositesb.2019.107607.

[13] Kadhim BB. Ablation characteristics of TiO2/UPE-PMMA blend nanocomposites: empirical and simulation approaches. Energy Procedia 2017;119:718−22. https://doi.org/10.1016/j.egypro.2017.07.099.

[14] Kim JH, Kwon DJ, Shin PS, Baek YM, Park HS, DeVries KL, et al. The evaluation of the interfacial and flame retardant properties of glass fiber/unsaturated polyester composites with ammonium dihydrogen phosphate. Compos B Eng 2019;167:221−30. https://doi.org/10.1016/j.compositesb.2018.12.032.

[15] Qin R, Song Y, Niu M, Xue B, Liu L. Construction of flame retardant coating on polyester fabric with ammonium polyphosphate and carbon microspheres. Polym Degrad Stabil 2019;171:109028. https://doi.org/10.1016/j.polymdegradstab.2019.109028.

[16] Munir MJ, Kazmi SMS, Wu YF, Hanif A, Khan MUA. Thermally efficient fired clay bricks incorporating waste marble sludge: an industrial-scale study. J Clean Prod 2018;174:1122−35. https://doi.org/10.1016/j.jclepro.2017.11.060.

[17] Sutcu M, Alptekin H, Erdogmus E, Er Y, Gencel O. Characteristics of fired clay bricks with waste marble powder addition as building materials. Construct Build Mater 2015;82:1−8. https://doi.org/10.1016/j.conbuildmat.2015.02.055.

[18] Saboya F, Xavier GC, Alexandre J. The use of the powder marble by-product to enhance the properties of brick ceramic. Construct Build Mater 2007;21:1950−60. https://doi.org/10.1016/j.conbuildmat.2006.05.029.

[19] Pappu A, Thakur VK, Patidar R, Asolekar SR, Saxena M. Recycling marble wastes and Jarosite wastes into sustainable hybrid composite materials and validation through Response Surface Methodology. J Clean Prod 2019;240:118249. https://doi.org/10.1016/j.jclepro.2019.118249.

[20] Khyaliya RK, Kabeer KISA, Vyas AK. Evaluation of strength and durability of lean mortar mixes containing marble waste. Construct Build Mater 2017;147:598−607. https://doi.org/10.1016/j.conbuildmat.2017.04.199.

[21] Binici H, Aksogan O. Durability of concrete made with natural granular granite, silica sand and powders of waste marble and basalt as fine aggregate. Journal of Building Engineering 2018;19:109−21. https://doi.org/10.1016/j.jobe.2018.04.022.

[22] Aydin E, Arel HŞ. High-volume marble substitution in cement-paste: towards a better sustainability. J Clean Prod 2019;237:117801. https://doi.org/10.1016/j.jclepro.2019.117801.

[23] Çınar ME, Kar F. Characterization of composite produced from waste PET and marble dust. Construct Build Mater 2018;163:734−41. https://doi.org/10.1016/j.conbuildmat.2017.12.155.

[24] Souza F, Bragança SR. Thermogravimetric analisys of limestones with different contents of MgO and microstructural characterization in oxy-combustion. Thermochim Acta 2013;561:19−25. https://doi.org/10.1016/j.tca.2013.03.006.

[25] Barcina LM, Espina A, Suárez M, García JR, Rodríguez J. Characterization of monumental carbonate stones by thermal analysis (TG, DTG and DSC). Thermochim Acta 1997;290(2):181−9. https://doi.org/10.1016/S0040-6031(96)03074-2.

[26] Gomes Ribeiro CE, Sánchez Rodriguez RJ. Influence of compaction pressure and particle content on thermal and mechanical behavior of artificial marbles with marble waste and unsaturated polyester. Mater Res 2015;18(Suppl 2):283−90. https://doi.org/10.1590/1516-1439.372314.

[27] Hobart M. King Marble: a non-foliated metamorphic rock that forms when limestone is subjected to heat and pressure Available online: https://geology.com/rocks/marble.shtml (accessed 9 November 2020).

[28] Rudin A, Choi P. The elements of polymer science and engineering. 3rd ed. Massachusetts: Academic Press; 2013.

[29] Nayak SK, Satapathy A. Development and characterization of polymer-based composites filled with micro-sized waste marble dust. Polym Polym Compos 2020;xx:1−12. https://doi.org/10.1177/0967391120926066.

[30] Nayak SK, Satapathy A, Mantry S. Processing and wear response study of glass-polyester composites with waste marble dust as particulate filler. Polym Compos 2020;41:2263−73. https://doi.org/10.1002/pc.25537.

[31] Dholakiya B. Unsaturated polyester resin for speciality applications [online]. In: Polyester; 2012. p. 167−202. https://www.intechopen.com/books/polyester/unsaturated-polyester-resin-for-specialty-applications. [Accessed 15 November 2020]. accessed.

[32] Feroca available online: https://www.feroca.com/en/polyester-resins/63-ferpol-3501-cv25-coladas-.html (accessed 17 November 2020).

[33] Reis JML. Effect of aging on the fracture mechanics of unsaturated polyester based on recycled PET polymer concrete. Mater Sci Eng 2011;528:3007−9. https://doi.org/10.1016/j.msea.2010.12.073.

[34] Yue T, Wahab MA. A numerical study on the effect of debris layer on fretting wear. Materials 2016;9:597. https://doi.org/10.3390/MA9070597.

[35] Harvoort G, van Reijen L. Measurement of the thermal conductivity of solid substances by DSC. Termochimica Acta 1965;93:317−20.

[36] Riesen R. Simple determination of the thermal conductivity of polymers by DSC. Mettler Toledo UserCom 2005;22:19−23.

[37] Abenojar J, de Armentia SL, Gálvez P, Martínez MA. Tribological and mechanical properties of polyester based

composites with SiC particles. In: Abdel Wahab M, editor. Proceedings of the 7th international conference on fracture fatigue and wear. FFW 2018. Lecture notes in mechanical engineering. Singapore: Springer; 2019. https://doi.org/10.1007/978-981-13-0411-8_70.

[38] Benzannache N, Bezazi A, Bouchelaghem H, Boumaaza M, Amziane S, Scarpa F. Statistical analysis of 3-point bending properties of polymer concretes made from marble powder waste, sand grains, and polyester resin. Mech Compos Mater 2018;53/6:781—90. https://doi.org/10.1007/s11029-018-9703-2.

[39] Mansour R, El Abidine RZ, Brahim B. Performance of polymer concrete incorporating waste marble and alfa fibers. Advanced Concrete Construction 2017;5:331—43. https://doi.org/10.12989/acc.2017.5.4.331.

[40] Fartini MS, Abdul Majid MS, Afendi M, Amin NAM, Mohamad A. Effects of elevated temperatures on the compression strength of nanoclay filled unsaturated polyester resin. Appl Mech Mater 2014;554:208—12. https://doi.org/10.4028/www.scientific.net/AMM.554.208.

[41] Mohamed MA, Moh MA, Akasha NM, Elgady IYI. Experimental study on effects of fiberglass and fiber waste in concrete mixes. International Journal of Engineering Sciences & Research Technology 2016;5(10):485—93. https://doi.org/10.5281/zenodo.160884.

[42] Bhatia S, Khan S, Angra S. Dry sliding wear characterization of SGM/boron carbide hybrid polymer matrix composite. Polym Polym Compos 2020; August 26:1—10. https://doi.org/10.1177/0967391120952593.

[43] Abenojar J, del Real JC, Martinez MA, Cano de Santayana M. Effect of silane treatment on SiC particles used as reinforcement in epoxy resins. J Adhes 2009;85:287—301. https://doi.org/10.1080/00218460902880131.

[44] Abenojar J, Martínez MA, Pantoja M, Velasco F, del Real JC. Epoxy composite reinforced with nano and micro SiC particles: curing kinetics and mechanical properties. J Adhes

2012;88:418—34. https://doi.org/10.1080/00218464.2012.660396.

[45] Abenojar J, Tutor J, Ballesteros Y, del Real JC, Martínez MA. Erosion-wear, mechanical and thermal properties of silica filled epoxy nanocomposites. Compos B Eng 2017;120:42—53. https://doi.org/10.1016/j.compositesb.2017.03.047.

[46] Fernández-Álvarez M, Velasco F, Bautista A. Effect on wear resistance of nanoparticles addition to a powder polyester coating through ball milling. J Coating Technol Res 2018;15:771—9. https://doi.org/10.1007/s11998-018-0106-z.

[47] Friedrich K. Microstructural efficiency and fracture toughness of short fiber/thermoplastic matrix composites. Compos Sci Technol 1985;22:43—74. https://doi.org/10.1016/0266-3538(85)90090-9.

[48] Hutchings IM. Tribology, friction and wear of engineering materials. In: Metallurgy and materials science. London: Edward Arnold; 1992.

[49] Abenojar J, Enciso B, Martinez M, Velasco F. Wear resistance of polypropylene-SiC composite. In: IOP publishing ltd; 6th international conference on fracture fatigue and wear 26—27 july 2017, porto, Portugal. Journal of physics: conference series. vol. 843; 2017, 012066.

[50] Tibiletti L, Longuet C, Ferry L, Coutelen P, Mas A, Robin JJ, et al. Thermal degradation and fire behaviour of unsaturated polyesters filled with metallic oxides. Polym Degrad Stabil 2011;96:67—75. https://doi.org/10.1016/j.polymdegradstab.2010.10.015.

[51] Sharma A, Patnaik A. Experimental investigation on mechanical and thermal properties of marble dust particulate-filled needle-punched nonwoven jute fiber/epoxy composite. J Miner Met Mater Soc 2018;70:1284—8. https://doi.org/10.1007/s11837-018-2828-x.

[52] Abenojar J, Pantoja M, Martínez MA, del Real JC. Aging by moisture and/or temperature of epoxy/SiC composites: thermal and mechanical properties. J Compos Mater 2015;49:2963—75. https://doi.org/10.1177/0021998314558496.